

pubs.acs.org/acscatalysis Research Article

Cobalt-Catalyzed Additive-Free Dehydrogenation of Neat Formic Acid

Bedraj Pandey, Jeanette A. Krause, and Hairong Guan*



Cite This: ACS Catal. 2024, 14, 13781-13791



Read Online

ACCESS I

Metrics & More

Article Recommendations

Supporting Information

ABSTRACT: Dehydrogenation of formic acid without using additives and solvents is a challenging research problem in base metal catalysis. In this study, cobalt complexes of the type ($^{iP}PP^RP$)CoH(PMe₃) ($^{iP}PP^RP = (o^{-i}Pr_2PC_6H_4)_2PR$; R = H or Me) are shown to catalyze the additive-free dehydrogenation of neat formic acid to carbon dioxide. The $^{iP}PP^{Me}P$ -ligated cobalt hydride is particularly effective, giving catalytic turnover numbers of up to 7122 with a single load of formic acid and 10,338 with a continuous addition of formic acid. Mechanistic investigation focusing on ($^{iP}PP^{Me}P$)CoH(PMe₃) reveals that the hydride complex is initially converted to [($^{iP}PP^{Me}P$)CoH₂(PMe₃)]⁺ and then to "($^{iP}PP^{Me}P$)Co-(OCHO)" as the key intermediates for releasing H₂ and CO₂, respectively. As the catalytic reaction proceeds, decarbonylation of formic acid produces CO, which transforms the intermediates to [($^{iP}PP^{Me}P$)Co(CO)(PMe₃)]⁺ and ($^{iP}PP^{Me}P$)Co-

P(Pr)₂
PMe₃
PCo H CO₂ + H₂
HCO₂H
P(Pr)₂
(R = H, Me)
base metal catalysts
no additives and no solvents
TONs up to 7122 (single batch)
and 10,338 (continuous addition)
neat acid is better than diluted acid

(CO)H as the less active forms of the catalyst. Further degradation to $[(^{iPr}PP^{Me}P)Co(CO)_2]^+$, protonated phosphine ligands, and cobalt formate ends the catalyst's life. Contrary to many other catalytic systems, the cobalt catalysts described here are more active in neat formic acid than in formic acid solutions, which can be attributed to the removal of PMe₃ from the coordination sphere (via phosphine protonation) to generate a more reactive intermediate.

KEYWORDS: base metal catalysis, hydrogen-storage material, formic acid, dehydrogenation, decarboxylation, decarbonylation, hydride complexes, cobalt catalysts

INTRODUCTION

The search for new molecular catalysts capable of releasing H₂ from formic acid under mild conditions has been a burgeoning area of research for years, largely driven by the prospect of using formic acid as a chemical hydrogen-storage material. Despite the progress made, the vast majority of the catalytic systems developed to date require dilution with a solvent and, in some cases, also a substantial amount of additive(s) for the dehydrogenation process to run efficiently. While effective, the incorporation of solvents and additives inevitably reduces system-based net volumetric and gravimetric hydrogen-storage capacities, which have upper limits of 53 g H₂/L and 4.4 wt % H₂, respectively, as calculated based on pure formic acid. Additionally, volatile solvents and additives (e.g., amines) can contaminate the gaseous products, thus increasing the costs associated with gas purification prior to fuel cell applications. ^{1h}

The formidable challenge for performing dehydrogenation of *neat* formic acid is to identify a catalyst that can maintain its structural integrity in a reasonably acidic medium. Moreover, without a solvent, the conversion of formic acid to H₂ and CO₂ becomes less thermodynamically favorable, ⁴ presumably due to the energy penalty paid to break the more elaborate hydrogenbonding network present in pure formic acid. ⁵ Nevertheless, Williams and co-workers successfully designed a P,N-ligated iridium complex (Chart 1) as a dehydrogenation (pre)catalyst

operable in neat formic acid, provided that a base such as HCO₂Na (5 mol %, relative to formic acid) is also added to the system.⁶ The catalytic reaction was conducted at 90 °C with a turnover number (TON) of 12,530 achieved in 13 h and a cumulative TON of 2,160,000 obtained over 4 months following 40 successive additions of formic acid. Since then, several other iridium-based catalysts have been developed, including Gelman's pincer-type complex bearing dangling NH₂ groups, Iglesias and Oro's diene complex supported by an Nheterocyclic olefin scaffold,8 and Fischmeister's Cp*Ir complexes containing a dipyridylamine ligand. 9,10 Very recently, Chen, Basset, and Huang have grafted a P,N,Pligated iridium trihydride on a fibrous silica nanosphere, which can be used to catalyze the dehydrogenation of neat formic acid with not only high TONs (up to 540,000) but also high turnover frequencies (up to 13,290 h⁻¹).¹¹ The immobilized catalyst shows improved activity over the homogeneous catalyst, although both require HCO₂Cs (12.5 mol %) to be

Received: July 10, 2024 Revised: August 16, 2024 Accepted: August 25, 2024 Published: August 31, 2024





Chart 1. Molecular Catalysts Developed for the Dehydrogenation of Neat Formic Acid

effective. Beyond iridium systems, Milstein's ruthenium hydride⁴ and Casado's cationic rhodium complex¹² prove to be efficient in catalyzing the dehydrogenation reaction under neat conditions. The ruthenium catalyst, in particular, is incredibly robust in hot formic acid (95 °C), producing H_2 and CO_2 with TONs up to 1,701,150.

The work presented herein addresses the following unsolved problem in catalytic dehydrogenation of formic acid: using a first-row transition metal instead of a precious metal to promote the reaction without the need of dilution and additive(s). Such a task is inherently more difficult to do because, with the 3d-series, the metal—ligand bonds are more ionic¹³ and thus more susceptible to attack by an acid to trigger catalyst degradation. In an early study, Ravasio employed a few copper compounds including simple salts (Chart 2) to catalyze the dehydrogenation of formic acid.¹⁴

Chart 2. Selected Catalysts Based on First-Row Transition Metals

The reaction was not diluted by a conventional solvent; however, it was carried out in formic acid that was substantially neutralized by an amine (e.g., 1 equiv of NEt₃). In addition, the obtained TONs were generally low (up to 72). Around the same time, Enthaler and Junge investigated the dehydrogenation of HCO₂H-"OctNMe₂ (in an 11:10 ratio) catalyzed by a nickel pincer hydride complex.¹⁵ The catalytic reaction was found to be more efficient when propylene carbonate (PC) was used as the solvent; without dilution, the TONs (up to 626 for the reaction in PC) dropped by ~60%. We made a

similar observation in a recent study of additive-free dehydrogenation of formic acid catalyzed by an iron dihydride complex. When the reaction medium was changed from 1,4-dioxane to neat formic acid, the TON decreased sharply from 864 to 67. In this work, we report significantly more active catalysts for the dehydrogenation of neat formic acid without using any additives. The new catalytic system features cobalt hydrides supported by a tridentate P,P,P-type ligand along with PMe₃, which, to our surprise, perform even better under the undiluted conditions.

■ RESULTS AND DISCUSSION

Synthesis of Cobalt Hydride Complexes. The target compound (${}^{\text{IP}}\text{rPP}^{\text{H}}\text{P}$)CoH(PMe₃) (1) was prepared through a ligand substitution reaction between HCo(PMe₃)₄ and ${}^{\text{IP}}\text{rPP}^{\text{H}}\text{P}$ (abbreviation for ($o^{-i}\text{Pr}_2\text{PC}_6\text{H}_4$)₂PH) carried out at 80 °C for 48 h (eq 1 see Supporting Information). Its *P*-methyl analog

$$P(^{i}Pr)_{2}$$

$$PR + HCo(PMe_{3})_{4} + \frac{toluene}{heating}$$

$$- 3PMe_{3}$$

$$- 3PMe_{3}$$

$$P(^{i}Pr)_{2}$$

$$- 3PMe_{3}$$

$$P(^{i}Pr)_{2}$$

$$R = H (1), Me (2)$$

 $(^{iPr}PP^{Me}P)CoH(PMe_3)$ (2) was synthesized similarly, although a higher temperature (100 °C) and a longer reaction time (72 h) were required Supporting Information. The displacement of three PMe₃ ligands by a P,P,P-type ligand was evident in the ³¹P{¹H} NMR spectra of the isolated products, each showing two broad resonances in the 60-100 ppm region attributable to the tridentate ligand and another broad resonance near -6ppm for the remaining PMe₃ ligand. The ³¹P-³¹P splitting is likely obscured by the quadrupolar ⁵⁹Co nucleus, which has been previously observed with other cobalt complexes involving different phosphorus-based donor groups. 17 The hydride resonance is, however, well resolved, featuring a doublet of apparent quartets at -13.83 ppm for 1 or -14.00 ppm for 2 (both dissolved in C_6D_6). The presence of a hydride ligand was also supported by the IR data, which showed a stretching vibration expected for a molecule bearing a metalhydrogen bond (1: 1828 cm⁻¹; 2: 1829 cm⁻¹).

The molecular structures of 1 and 2 were further studied by X-ray crystallography (Figure 1, see Supporting Information

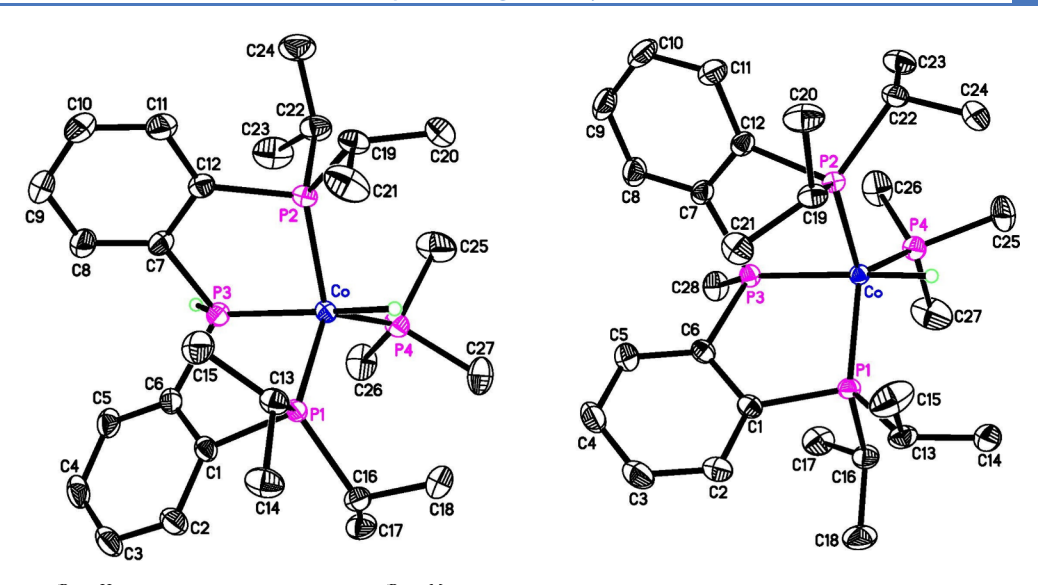


Figure 1. ORTEP of (^{iP}TPPHP)CoH(PMe₃) (1, left) and (^{iP}TPPMeP)CoH(PMe₃) (2, right) at the 50% probability level (all hydrogen atoms except the ones bound to phosphorus and cobalt are omitted for clarity). Selected bond lengths (Å) and angles (deg) in 1: Co-H 1.463(14), P-H 1.345(15), Co-P1 2.1488(3), Co-P2 2.1471(3), Co-P3 2.1037(3), Co-P4 2.1638(3); P1-Co-P2 125.939(13), P1-Co-P4 119.217(13), P2-Co-P4 113.748(14), P1-Co-P3 86.361(13), P2-Co-P3 86.456(13), P3-Co-P4 109.025(14). Selected bond lengths (Å) and angles (deg) in 2: Co-H 1.453(18), Co-P1 2.1479(3), Co-P2 2.1463(3), Co-P3 2.1150(3), Co-P4 2.1587(4); P1-Co-P2 124.451(14), P1-Co-P4 118.405(14), P2-Co-P4 116.051(14), P1-Co-P3 87.949(13), P2-Co-P3 87.172(13), P3-Co-P4 106.163(14).

Table 1. Cobalt-Based (Pre)Catalysts Developed for the Dehydrogenation of Formic Acid

Catalyst	Substrate	Solvent	Conditions	TONs	Ref			
$HCo{PPh(OEt)_2}_4$	HCO₂H	THF	30 °C, h <i>v</i> , 3−6 h	1.6-3.1	20			
(PhPNHP)CoCl	$HCO_2H-DMOA^a$ (11:10)	_	80 °C, 1.5 h	2260	21a			
(PhPNHP)CoCl ₂ -NaBEt ₃ H (1:2)	HCO ₂ H-HCO ₂ K (2:1 to 1:4)	H_2O	60 °C, 1−3 h	146-918	21a			
$(^{Cy}PP^{NHBn}P)Co(CO)H$	HCO₂H	1,4-dioxane, toluene, or H ₂ O	80 °C, 1−6 h	102-454	22			
$[(triphos)Co(CH_3CN)_2]^{2+}$	HCO ₂ H or HCO ₂ H-base (10:1)	CH ₃ CN	70 °C, 3−18 h	164-1735	21b			
a DMOA = $N_{i}N_{i}$ -dimethyloctylamine.								

for additional X-ray crystallographic information of 1 and 2). Apart from the substituent on the central phosphorus (H vs Me), structural variations between the two cobalt hydride complexes are negligible. Compared to our previously reported cis-(^{iPr}PP^HP)Fe(CO)H₂¹⁶ and cis-(^{iPr}PP^{Me}P)Fe(CO)H₂, the P,P,P-type ligands in the cobalt system adopt a more folded conformation. This is manifested by much smaller P1-M-P2 angles (125.939(13)° in 1 vs 152.444(16)° in cis-(iPrPPHP)- $Fe(CO)H_2$; 124.451(14)° in 2 vs 151.157(14)° or 154.667(14)° in cis-(iPrPPMeP)Fe(CO)H₂) and a noticeably smaller C6-P3-C7 angle $(104.73(6)^{\circ} \text{ in } 1 \text{ vs } 109.18(6)^{\circ} \text{ in }$ cis-(iPrPPHP)Fe(CO)H₂; 105.94(6)° in 2 vs 108.40(5)° or 109.17(5)° in cis-(iPrPPMeP)Fe(CO)H₂). The calculated geometry indices¹⁹ (1: $\tau_5 = 0.65$; 2: $\tau_5 = 0.71$) suggest that cobalt is situated in a distorted trigonal bipyramidal coordination sphere, where the central phosphorus and the hydride occupy the axial positions (P3-Co-H angle: $164.7(6)^{\circ}$ in 1; $167.2(7)^{\circ}$ in 2). Another structural feature worth noting is that PMe3 is syn to the PH hydrogen in 1 or the PMe methyl group in 2. Nuclear Overhauser effect spectroscopy (NOESY) experiments with 1 and 2 (in C_6D_6)

also showed these correlations through space, suggesting that the *syn* configuration is preserved in solution.

The two cobalt hydride complexes are air-sensitive compounds. When exposed to air, the red solution samples of 1 and 2 (in C_6D_6) quickly turned turbid and then formed a brown precipitate. Under an inert atmosphere, thermal decomposition started to occur when a solution of 1 in toluene- d_8 was heated at 100 °C for 24 h, signaled by the formation of a small amount of free PMe₃ (<5%). The methylated derivative 2 is thermally more stable; at a higher temperature of 120 °C, its toluene- d_8 solution did not show any sign of degradation (monitored for 24 h).

Catalytic Activity. Prior to this work, several cobalt complexes were already reported to catalyze the dehydrogenation of formic acid. As summarized in Table 1, these catalytic systems require photoirradiation²⁰ or a significant amount of base²¹ and, to the best of our knowledge, were tested only with diluted formic acid. Of particular interest and relevance are the studies of PhPNHP-ligated Co^I and Co^{II} complexes^{21a} and (CyPPNHBnP)Co^I(CO)H,²² in which the NH functionality was proposed to play crucial roles in stabilizing some of the

catalytic intermediates via N–H···O hydrogen-bonding interactions. However, $[(\text{triphos})\text{Co}^{II}(\text{CH}_3\text{CN})_2]^{2^+}$ is also a competent catalyst despite the fact that it lacks an NH group needed to participate in the interactions from the secondary coordination sphere. Regardless of the differences in ligand structure and metal oxidation state, the unifying theme of these catalytic systems is the involvement of a cobalt hydride intermediate.

With the hydride already bound to cobalt, 1 and 2 were expected to be active catalysts for the dehydrogenation reaction. To understand the solvent effects, catalytic activity was first studied using pure formic acid diluted with different solvents. As shown in Table 2, the reaction is best carried out in nonpolar solvents. The use of *n*-octane, in particular, led to successful dehydrogenation of formic acid with the first-hour TONs of 302 for 1 (entry 1) and 377 for 2 (entry 9). Extending the reaction time resulted in further increase of TONs up to 355 for 1 and 413 for 2. The reaction conducted

Table 2. Cobalt-Catalyzed Dehydrogenation of Formic Acid Under Diluted Conditions^a

$$HCO_2H \xrightarrow{0.1 \text{ mol}\% [Co]} H_2 + CO_2$$

Entry	Catalyst	Solvent + Additive	$(\text{conv.})^{e,f}$	TON _{max} (time, conv.)
1	${{(^{iPr}PP^{H}P)}\atop{CoH(PMe_{3})}}$ (1)	n-octane	302 (30%)	355 (3 h, 36%)
2	$({}^{iPr}PP^{H}P)$ CoH(PMe ₃) (1)	toluene	117 (12%)	276 (3 h, 28%)
3	$ \begin{array}{c} (^{iPr}PP^{H}P) \\ CoH(PMe_{3}) \ (1) \end{array} $	1,4-dioxane	15 (2%)	15 (1 h, 2%)
4	${{}^{(i^{Pr}PP^{H}P)} \atop {CoH(PMe_{3})}}$ (1)	<i>t</i> -butyl alcohol	15 (2%)	15 (1 h, 2%)
5	${(^{iPr}PP^{H}P)}$ CoH(PMe ₃) (1)	propylene carbonate	98 (10%)	98 (1 h, 10%)
6	$({}^{iPr}PP^{H}P)$ CoH(PMe ₃) (1)	DMSO	8 (<1%)	8 (1 h, < 1%)
7 ^b	$({}^{iPr}PP^{H}P)$ CoH(PMe ₃) (1)	<i>n</i> -octane + NEt ₃	87 (9%)	87 (1 h, 9%)
8 ^c	$(^{iPr}PP^{H}P)$ CoH(PMe ₃) (1)	<i>n</i> -octane + LiBF ₄	336 (34%)	435 (3 h, 44%)
9	$(^{iPr}PP^{Me}P)$ CoH(PMe ₃) (2)	<i>n</i> -octane	377 (38%)	413 (2 h, 41%)
10	$ \begin{array}{c} \left(^{iPr}PP^{Me}P\right) \\ CoH(PMe_3) (2) \end{array} $	toluene	356 (36%)	356 (1 h, 36%)
11	$(^{iPr}PP^{Me}P)$ CoH(PMe ₃) (2)	1,4-dioxane	8 (<1%)	8 (1 h, < 1%)
12	$ \begin{array}{c} \left(^{iPr}PP^{Me}P\right) \\ CoH(PMe_3) (2) \end{array} $	<i>t</i> -butyl alcohol	12 (1%)	12 (1 h, 1%)
13	$(^{iPr}PP^{Me}P)$ CoH(PMe ₃) (2)	propylene carbonate	97 (10%)	97 (1 h, 10%)
14	${{(^{iPr}PP^{Me}P)} \choose {CoH(PMe_3)}}$ (2)	DMSO	8 (<1%)	8 (1 h, < 1%)
15 ^b	$ \begin{array}{c} {^{(i^{Pr}PP^{Me}P)}} \\ {^{CoH(PMe_3)}(2)} \end{array} $	<i>n</i> -octane + NEt ₃	449 (45%)	845 (5 h, 85%)
16 ^c	$({}^{iPr}PP^{Me}P)$ CoH(PMe ₃) (2)	<i>n</i> -octane + LiBF ₄	577 (58%)	608 (2 h, 61%)
17 ^d	$(^{iPr}PP^{Me}P)$ CoH(PMe ₃) (2)	<i>n</i> -octane	349 (35%)	372 (2 h, 37%)

^aStandard conditions: HCO₂H (100 μL, 98–100% purity, 2.65 mmol) and a cobalt catalyst (0.00265 mmol, 0.1 mol %) mixed in a solvent (0.5 mL). ^bNEt₃ (100 mol %) was added. ^cLiBF₄ (10 mol %) was added. ^dDCO₂D was employed as the substrate. ^eTON_{1h} is the turnover number obtained after 1 h. ^fAverage of two runs. ^gTON_{max} is the turnover number obtained when the gas production ceased.

in a polar solvent such as 1,4-dioxane and propylene carbonate typically stopped after 1 h with considerably lower TONs (<100). These results presumably reflect the rates at which the catalysts degrade in different solvents. Evidently, base additives are not always beneficial to the catalytic process. Adding 1 equiv of NEt₃ to formic acid accelerated the deactivation of 1 (entry 7) but extended the lifetime of 2 (entry 15). In the latter case, a maximum TON of 845 was obtained. For some catalytic systems, Lewis acids such as LiBF4 can enhance the performance of the catalysts by stabilizing the intermediates/ transition states involved in the decarboxylation step. 2a,23 While studying cis-(iPrPPHP)Fe(CO)H₂¹⁶ and cis-(iPrPPMeP)-Fe(CO)H₂, we found that LiBF₄ was detrimental to the ironcatalyzed dehydrogenation of formic acid. Thus, the roles played by the Lewis acids can be multifaceted and complicated. For the cobalt system studied here, adding LiBF₄ (10 mol %) to the reaction mixture showed some improvement as far as the TONs are concerned (entry 8 vs entry 1; entry 16 vs entry 9). Finally, when DCO₂D was employed as the substrate, the first-hour TON and the maximum TON decreased slightly (entry 17 vs entry 9), indicating that the nominal KIE is small

As discussed in the Introduction, a more attractive catalytic system would be the one that can operate in neat formic acid without additives. Counterintuitively, 1 and 2 displayed a much higher activity under such conditions (Figure 2A). When the initial HCO₂H:1 ratio was set to 10,000, a steady gas evolution was observed within the first 3 h of heating (80 °C) but became sluggish afterward with the TON plateaued at 1595. The methylated derivative 2 proved to be a more efficient catalyst, giving a TON of 1062 for the first hour and a maximum TON of 7122 after 9 h. This translates to a 71% conversion of the formic acid, which is close to the upper limit due to condensation of formic acid in places beyond the reach of the catalyst. The composition of the gaseous products was analyzed by gas chromatography (GC) as a 51:49 mixture of H₂ and CO₂ contaminated by a trace of CO (0.07%). In an effort to maximize the TON, a second load of formic acid was added to the aforementioned reaction with 2 at the 9 h mark, which produced more gas but merely for 1 h with an additional TON of 372 (i.e., with a cumulative TON of 7494). Increasing the initial HCO₂H:2 ratio to 20,000 or 100,000 resulted in diminished TONs (<2000, see Table S1 in the Supporting Information), suggesting that catalyst deactivation is faster at a lower concentration. The dehydrogenation reaction was also performed by premixing HCO₂H with 2 in a 5,000 ratio, followed by a continuous addition of HCO₂H at a rate of 0.1 mL/h to mimic continuous flow conditions. This resulted in a TON of 1085 for the first hour and a maximum TON of 10,338 after 20 h. It is well-known that formic acid readily forms an azeotropic mixture with water, and the removal of water to obtain formic acid with a high purity requires additional energy input.²⁴ We found that the cobalt catalytic system was amenable to low-grade formic acid with a water content of ~12%, which generated a reaction profile very similar to that of pure formic acid (Figure 2B). For formic acid to be used as an energy carrier, it is also desirable to produce high-pressure $H_2^{4,25}$ which can be problematic with many catalytic systems. Our dehydrogenation reaction carried out in a closed system showed that the pressure eventually reached 250 psig or 18.2 bar (Figure 2C).

Active Forms of the Catalysts. To probe the mechanistic details, NMR experiments were first conducted using a

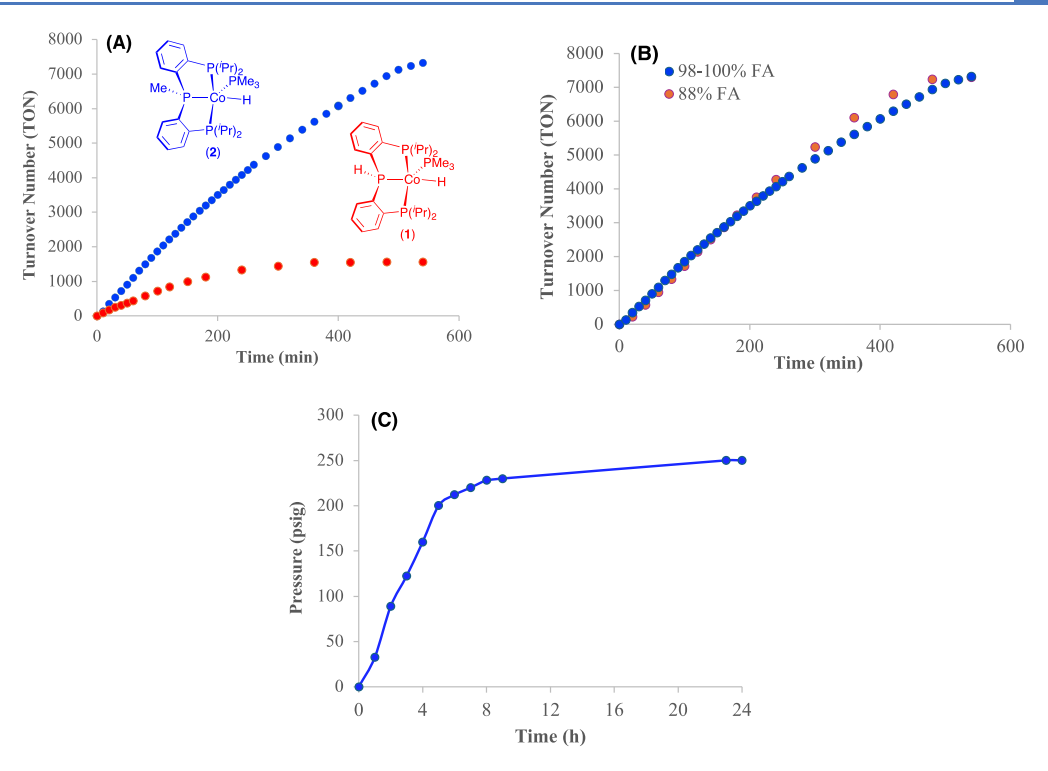


Figure 2. Reaction profiles for the cobalt-catalyzed additive-free dehydrogenation of formic acid (26.5 mmol HCO_2H , 0.01 mol % catalyst loading, 80 °C). (A) Comparison between the two cobalt hydrides. (B) Effect of formic acid (FA) purity on the reaction catalyzed by 2. (C) Pressure changes during the dehydrogenation of neat formic acid catalyzed by 2 (performed in a closed 25 mL Parr reactor; corrections were made to account for the vapor pressure).

solution of 2 in C₆D₆ (8.8 mM) mixed with formic acid, which, to some extent, mimics the catalytic conditions applied to the diluted acid (Table 2). It was interesting to note that the NMR spectra recorded right after mixing showed clean formation of a new product (3) along with H₂ (4.47 ppm), as long as the amount of added formic acid was high (18 equiv). In contrast, when 5 equiv of formic acid were added, ~ 15% of 2 decomposed to the protonated iPrPPMeP ligand. 26 The different outcomes for these experiments may potentially explain why higher TONs were obtained with neat formic acid, although it remains unclear how the large excess of formic acid delays catalyst degradation. The observation of H2 hinted to us that 3 could be a neutral cobalt formate complex (iPrPPMeP)Co-(OCHO)(PMe₃) or a cationic complex [(iPrPPMeP)Co-(PMe₃)]⁺ with a formate counterion. Efforts to isolate this compound for further characterization were fruitless, in part due to the complication of further reactions (vide infra). The product generated in situ from 2 and formic acid (mixed in methanol) was quickly analyzed by electrospray ionization mass spectrometry (ESI-MS). The expected ion [(iPrPPMeP)- $Co(PMe_3)$]⁺ (m/z = 567.08) was observed; however, the dominant ion was found to be $[(^{iPr}PP^{Me}P)CoH_2(PMe_3)]^+$ (m/z = 569.08) with two more hydrogens. This data, coupled with the fact that cationic CoH2 species are well precedented in the literature, 17b,20,27 prompted us to search for spectroscopic evidence of a dihydrogen or dihydride complex. Although no hydride signal was detected upon mixing 2 with formic acid (18 equiv), cooling the sample (prepared in toluene- d_8 to avoid solvent freezing) to -25 °C rendered two broad resonances visible in the hydride region (-12.52 and -16.99 ppm). This dynamic behavior is reminiscent of our previously studied (iPrPPMeP)Fe(CO)H2 that bears two rapidly exchanged hydride ligands bound to iron in a cis configuration. 18 Taken

together, the ESI-MS and NMR data support the proposition that 3 is cis-[($^{\rm IP}$ PP $^{\rm Me}$ P)CoH₂(PMe₃)] $^+$ with a formate counterion, which likely interacts with formic acid via hydrogen bonds. In an attempt to isolate a more stable analog of 3, the cobalt hydride complex 2 was treated with acetic acid in large access. Unfortunately, the resulting product also decomposed during workup. In solution, it displayed similar NMR features as 3 and gave ESI-MS data nearly identical to 3. More importantly, its 1 H $^-$ 1H NOSEY NMR spectrum showed correlation between the PMe₃ and PMe hydrogens, confirming that the methyl substituent on the central phosphorus is cis to PMe₃.

Protonation of 2 with formic acid to yield 3 (Scheme 1) must be the first step of the catalytic cycle. Subsequent

Scheme 1. Protonation of 2 with Diluted Formic Acid at Room Temperature

$$\begin{array}{c} \text{Me.} & \text{P}(\text{Pr})_2 \\ \text{PP}(\text{Pr})_2 \\ \text{PP}(\text{Pr})_2 \\ \text{PP}(\text{Pr})_2 \\ \text{Ne.} & \text{PP}(\text{Pr})_2 \\ \text{PP}(\text{Pr})_2 \\ \text{Ne.} & \text{PP}(\text{PP})_2 \\ \text{Ne.} & \text{PP}(\text{PP})_$$

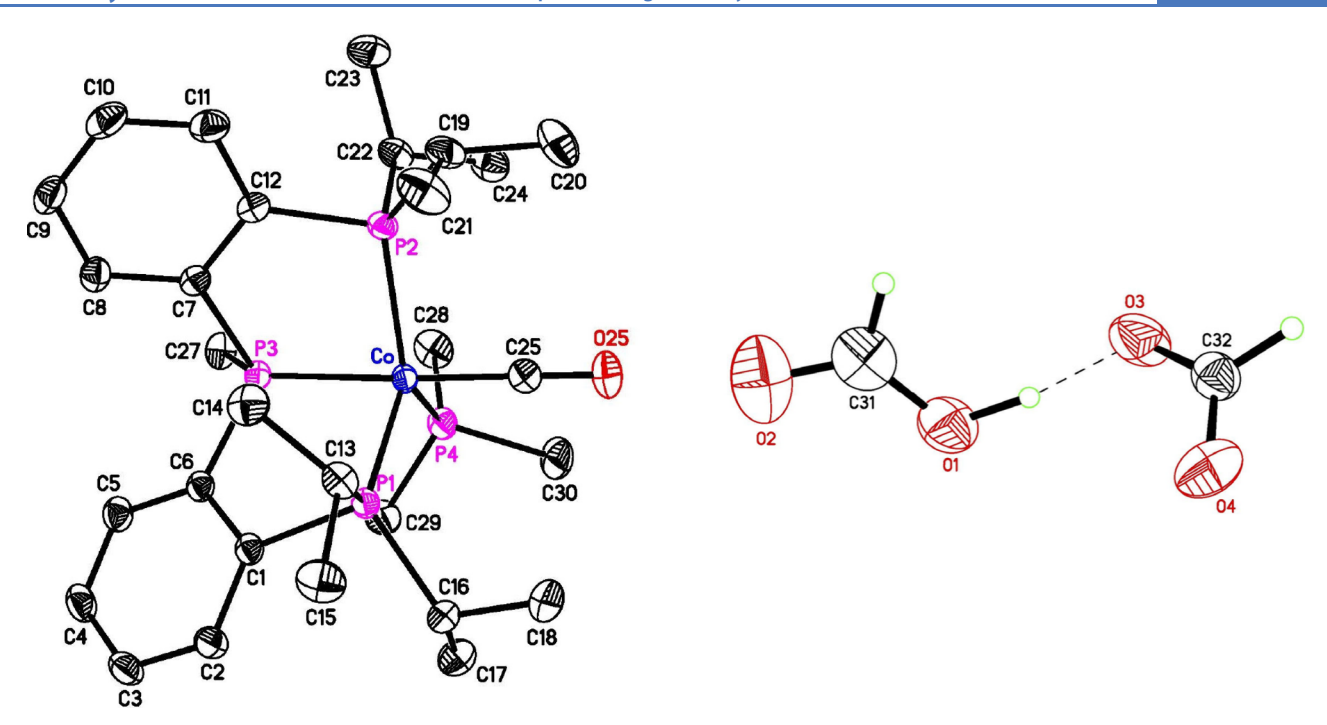


Figure 3. ORTEP of $[(^{iPr}PP^{Me}P)Co(CO)(PMe_3)][HCO_2H\cdots O_2CH]$ (5) at the 50% probability level (for clarity, all hydrogen atoms in the cation are omitted; the cation and the counterion are shown separately). Selected bond lengths (Å) and angles (deg): Co-P1 2.2255(4), Co-P2 2.2180(4), Co-P3 2.1800(4), Co-P4 2.2266(4), Co-C25 1.7387(15), C25-O25 1.1510(19); C25-Fe-P1 94.83(6), C25-Co-P2 92.94(5), C25-Co-P3 176.71(5), C25-Co-P4 90.54(5), P1-Co-P2 123.839(15), P1-Co-P4 112.609(15), P2-Co-P4 122.844(16), P1-Co-P3 85.620(14), P2-Co-P3 84.124(14), P3-Co-P4 92.291(15).

elimination of H_2 from cobalt would generate $[(^{iPr}PP^{Me}P)Co-(PMe_3)]^+$ with the formate ion residing outside and/or at the coordination sphere (4 and/or 4'). The room-temperature reaction favors the formation of 3, although upon heating H_2 elimination is expected to proceed more readily. The resulting product 4/4' should be poised to release CO_2 .

In fact, CO₂ (124.8 ppm) was detected by ¹³C{¹H} NMR spectroscopy from the reaction of 2 with H¹³CO₂H (6 equiv) carried out in C₆D₆, although at room temperature the decarboxylation process was slow. The ³¹P{¹H} NMR spectra for the reaction of 2 with HCO₂H were insightful, showing a slow conversion of 3 (~20% over 48 h) to another P,P,Pligated cobalt complex (5, Supporting Information). This new species formed cleanly when the reaction mixture was heated at 80 °C for 5 min. The ESI-MS analysis of the sample (diluted with methanol) revealed ions with m/z ratios of 594.83 and 519.17, which are consistent with [(iPrPPMeP)Co(CO)- (PMe_3)]⁺ and $[(^{iPr}PP^{Me}P)Co(CO)]$ ⁺, respectively. Single crystals were obtained from a separate experiment using toluene as the reaction medium and then layered with pentane. Crystallographic study of these crystals confirmed that 5 is indeed the cationic complex [(iPrPPMeP)Co(CO)(PMe3)]+ (Figure 3, see Supporting Information for additional X-ray crystallographic information of 5). As expected, 29 the formate counterion forms a strong hydrogen bond with formic acid $(O1-H\cdots O3 = 2.452(2) \text{ Å}, 170(3)^{\circ})$. The PMe₃ ligand maintains the syn configuration with respect to the PMe methyl group and the coordination geometry remains distorted trigonal bipyramidal (τ_5 = 0.88; P3-Co-C25 angle = $176.71(5)^{\circ}$). In addition to the substitution of H⁻ for CO, the main structural change involves the four Co-P bonds, which are elongated by 0.07-0.08 Å in comparison to the corresponding Co-P bonds in the hydride complex 2.

The formation of 5 suggests that formic acid may have undergone decarbonylation to provide the CO ligand for cobalt. This type of reactivity has been previously observed with H₂[RuCl₄]³⁰ and Milstein's ruthenium hydride⁴ shown earlier in Chart 1. An alternative pathway to generate CO is through a reduction of CO₂ with PMe₃, as demonstrated by the reaction of Cp*Mo(PMe₃)₃H with HCO₂H to give Cp*Mo(PMe₃)₂(CO)H, O=PMe₃, and H₂.³¹ It should be mentioned that O=PMe3 was not observed from our reaction of 2 with HCO₂H. Control experiments confirmed that ^{iPr}PP^{Me}P and PMe₃ were inert to CO₂ (1 bar, 80 °C, in C₆D₆). Treatment of these phosphine ligands with HCO₂H resulted in protonation instead of oxidation of the phosphorus centers. These results indicate that decarbonylation of formic acid must be the source of CO and this process is promoted by cobalt.

The cationic complex 5 proved to be a transient species on the reaction path started by 2 and formic acid (Scheme 2). Extending the heating time at 80 °C led to the disappearance of 5 and the formation of a new hydride species (6) along with

Scheme 2. Transformations of Catalyst 2 in Diluted Formic Acid under Heating

free PMe₃, a process that was not significantly accelerated by bubbling CO through the reaction mixture Supporting Information. This new hydride complex was isolated in an analytically pure form and characterized as ($^{iP}PP^{Me}P$)CoH-(CO). The most diagnostic NMR signal of 6 is the hydride resonance centered at -10.89 ppm as a doublet of triplets, which was further split when $H^{13}CO_2H$ was used as the substrate. In essence, the metal abstracts H^- from the formate ion but loses the PMe₃ ligand. The reaction of 2 with DCO₂D (\sim 6 equiv) at 80 °C generated the expected cobalt deuteride complex ($^{iP}PP^{Me}P$)CoD(CO) (6-D) as confirmed by 2H NMR spectroscopy, although extensive H/D scrambling was also observed with the gas product (H_2 , HD, and D_2), the cobalt hydride (6 and 6-D), and the monophosphine (PMe₃ and PMe₃-d_x). The crystal structure of 6 (Figure 4, see

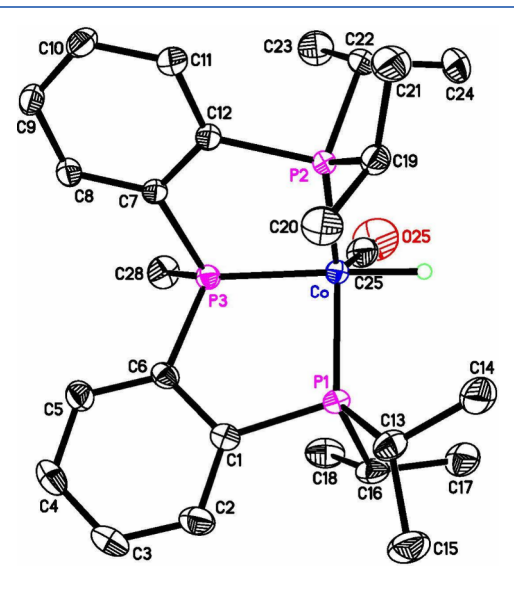


Figure 4. ORTEP of (*PPPMeP)CoH(CO) (6) at the 50% probability level (all hydrogen atoms except the one bound to cobalt are omitted for clarity). Selected bond lengths (Å) and angles (deg): Co-H 1.436(20), Co-P1 2.1654(3), Co-P2 2.1463(4), Co-P3 2.1137(4), Co-C25 1.7438(14), C25-O25 1.1562(18); P1-Co-P2 125.029(14), P1-Co-C25 117.92(5), P2-Co-C25 116.44(5), P1-Co-P3 88.538(13), P2-Co-P3 88.411(13), P3-Co-C25 101.53(5).

Supporting Information for X-ray crystallographic information of 6) shows that during this process there is also a *trans*-to-*cis* CO migration (relative to the central phosphorus). In converting 5 to 6, the distorted trigonal bipyramidal geometry about cobalt ($\tau_5 = 0.72$; P3–Co–H angle = $168.3(8)^\circ$) is preserved while the Co–P bonds are contracted to lengths comparable to those in 2.

The carbonyl-ligated cobalt hydride complex 6 still displayed some catalytic activity for the dehydrogenation of formic acid, albeit less efficiently. In n-octane at 80 °C, the dehydrogenation reaction catalyzed by 6 (0.1 mol % loading) gave a TON of 118 for the first hour and a maximum TON of 194 after 3 h. Comparing this result with one obtained for 2 under the same conditions (Table 2, entry 9) indicates that the catalytic activity has already diminished by >50%. The difference is even more pronounced for the catalytic dehydrogenation of neat formic acid (0.01 mol % loading). The measured TONs (TON_{1h} = 122, TON_{max} = 456) suggest that 6 is approximately 1 order of magnitude less active than 2.

To understand how the catalysts evolve in neat formic acid, 2 was dissolved in formic acid (HCO₂H:2 ratio = 1500) and the resulting sample was used directly for NMR analysis. Gas evolution started slowly at room temperature. The ³¹P{¹H} NMR spectrum recorded shortly after mixing showed three broad resonances at 98.2, 71.0, and -4.3 ppm (integrate to 2:1:1). These chemical shift values are reasonably close to those observed for the cationic cis-dihydride complex 3 (99.5, 73.0, and -3.2 ppm); the differences could arise from solvent effects (HCO₂H vs C₆D₆). Extending the reaction time to 48 h resulted in a partial conversion of the initially formed product to a new cobalt species 7 (89.6 and 77.7 ppm, integrate to 1:2) along with [HPMe₃]⁺ (-4.4 ppm). As one might have anticipated, gas evolution accelerated once the sample was heated at 80 °C. After 1 h of heating, the ³¹P{¹H} NMR spectrum displayed resonances mainly for 7 and [HPMe₃]⁺ with the initially formed cobalt product (3 or 3-like compound) representing ~10% of the total phosphoruscontaining species. A similar experiment performed with 2 in neat H¹³CO₂H confirmed that 7 does not contain a CO ligand and, at this stage, CO is not yet produced. A more rigorous characterization of these cobalt intermediates is challenging due to the complexity of the reaction and the difficulty to isolate them from neat formic acid. We propose that catalyst 2 is first protonated at the metal to form 3 (Scheme 3). In neat

Scheme 3. Postulated Reaction Sequence of 2 in Neat Formic Acid

formic acid, which is a more acidic medium, PMe₃ dissociation from 3 becomes more favorable, because protonation of the phosphorus lone pair drives this process. This provides a coordinatively unsaturated species that should make reductive elimination of H₂ more facile. Subsequent binding of the formate ion generates a 4-coordinate Co(I) complex that we tentatively assign as the structure of 7. In our studies of i^{Pr}PP^{Me}P-supported iron complexes, ^{18,26} we found that the central phosphorus could be upfield-shifted or downfield-shifted from the outer phosphorus, depending on the nature of the opposing ligand. The proposed structure of 7 agrees with our previous analysis that replacing a hydride ligand with a weakly *trans*-influencing ligand such as formate can result in a switch of the relative positions for the two phosphorus resonances.

Scheme 4. Catalyst Evolution during the Dehydrogenation of Formic Acid

Gas evolution continued at 80 $^{\circ}$ C until only a small amount of formic acid was left. The residue was dissolved in C_6D_6 for additional NMR analysis. The $^{31}P\{^1H\}$ NMR spectrum was surprisingly clean, showing only the resonances of 5. Formation of this cationic carbonyl complex was further supported by the $^{13}C\{^1H\}$ NMR spectrum of the ^{13}C -enriched sample, which revealed a multiplet around 221 ppm, the residual formic acid (165.2 ppm), and the dissolved CO_2 gas (124.8 ppm). This result leads to the conclusion that the use of neat formic acid cannot completely suppress CO formation but significantly delays the decarbonylation of formic acid.

Catalyst Deactivation. The NMR experiments described above provided snapshots of the cobalt catalysts in various active forms during the course of the dehydrogenation reaction. The catalytic reaction, whether carried out in solution or in neat formic acid, eventually ceased to operate as it approached the end of the catalyst's life. When gas evolution stopped, the reaction mixture turned cloudy and light in color. For a better understanding of the catalyst deactivation pathway, 2 was allowed to fully decompose in neat formic acid and then analyzed following extraction with C₆D₆. The ³¹P{¹H} NMR spectrum revealed that the soluble components consisted of the protonated iPrPPMeP and PMe3, some oxidation products and, most interestingly, a new iPrPPMePligated cobalt complex 8 (101.9 and 100.1 ppm, AB₂ spin, J_{AB} = 47.2 Hz). Efforts to purify and isolate this compound failed despite repeated trials. ESI-MS analysis of the C₆D₆ solution showed minor ions for the oxidized ligands and two major ions with m/z ratios of 547.00 and 519.17, which can be attributed to $[(^{iPr}PP^{Me}P)Co(CO)_2]^+$ and $[(^{iPr}PP^{Me}P)Co(CO)]^+$, respectively. The most plausible structure of 8 is thus the cationic dicarbonyl cobalt complex with $[(HCO_2)(HCO_2H)_x]^-$ as the counterion. This assignment is also consistent with the IR spectrum of the decomposed catalyst (prior to C_6D_6 extraction) that features two CO bands (2015 and 1971 cm⁻¹).

The solid left after C₆D₆ extraction (the insoluble components) exhibited a light pink color. Its IR spectrum showed bands at 1576, 1349, and 786 cm⁻¹ typical of stretching and deformation vibrations of a formate ligand. 32 Other bands present in the spectrum suggested that there was some formic acid left in the sample. The mechanistic study of formic acid dehydrogenation catalyzed by [(triphos)-Co^{II}(CH₃CN)₂]²⁺ also mentioned a pink precipitate being formed at the end of the catalytic process, 21b which was characterized crystallographically as the known compound Co(OCHO)₂·2H₂O. Our independently synthesized Co- $(OCHO)_2 \cdot 2H_2O$, however, displayed ν_{OCO} and δ_{OCO} bands (1555, 1371, 1354, 758, and 726 cm⁻¹) that did not match the bands for our decomposed catalyst (see Figures S37 and S38 in the Supporting Information). The discrepancy can be reconciled by the fact that cobalt formate exists as different coordination polymers, depending on the water content in the reaction mixture. In Co(OCHO)2.2H2O, each formate bridges two cobalt centers while the water molecules act as terminally bound ligands.³³ In anhydrous cobalt formate, each formate bridges three cobalt centers to construct a microporous metal organic framework (MOF). Given the relatively low moisture levels under our catalytic conditions, we think the decomposed catalyst should more closely resemble the anhydrous form of cobalt formate. To test this hypothesis, Co(OCHO)₂·2H₂O was heated in formic acid at 80 °C for an extended period of time (48 h), which was designed to displace the coordinated water molecules. The recovered materials and the decomposed catalyst indeed share common IR bands associated with the formate ligand. Minor differences could be due to impurities present in the two samples. In fact, the cobalt formate-based

MOF is known to trap various solvents (e.g., DMF, THF, CH₃CN, acetone), ³⁴ gas molecules (e.g., CO₂, CH₄, Xe)³⁵ and, most relevant to this work, formic acid along with a small amount of water. ³⁶

Considering that all the cobalt complexes discussed so far involve a Co(I) or Co(III) center, one might ask how Co^{II}(OCHO)₂ could even form during the reaction. We propose that the unsupported "Co^I(OCHO)" could undergo oxidative addition with formic acid to form HCo^{III}(OCHO), followed by the loss of H_2 to produce $Co^{II}(OCHO)_2$, although this needs to be further investigated. Formate salts sometimes can react with phosphine ligands to yield phosphine complexes, as exemplified by the formation of Ni(PMe₃)₄ from the reaction of Ni(OCHO)₂•2H₂O with PMe₃. However, no reaction was observed when Co-(OCHO)2•2H2O was treated with iPrPPMeP at 80 °C in C_6D_6 -THF or C_6D_6 -EtOH. The mechanistic implication of this result is that, once cobalt formate precipitates out of the reaction mixture, it is difficult to convert back to P,P,P-ligated complexes to rejuvenate the catalysts.

CONCLUSIONS

In summary, we have shown cobalt hydrides stabilized by a tridentate P,P,P-type ligand and PMe3 as catalysts for the dehydrogenation of formic acid to carbon dioxide. The catalytic system does not require additives or solvents. As a matter of fact, it displays a higher catalytic activity in neat formic acid than in formic acid diluted with a solvent. The observed catalytic turnovers (TONs up to 7122 for a single run and 10,338 with a continuous addition of formic acid) rank these cobalt hydrides as the most active cobalt catalysts known to date for formic acid dehydrogenation and the best basemetal catalysts that can operate under neat conditions. Our detailed mechanistic investigation focusing on (iPrPPMeP)CoH-(PMe₃) (2) suggests that formic acid first protonates the cobalt center to yield a cationic cis-dihydride complex (Scheme 4). Subsequent elimination of H₂ generates intermediates of the type "(iPrPPMeP)Co(OCHO)", which in turn undergo decarboxylation to release CO2. The advantage of using neat formic acid lies in the fact that the reaction medium is acidic enough to protonate PMe3. The resulting cobalt formate complex (7) presumably has a lower kinetic barrier for decarboxylation than the PMe₃-ligated formate species (4 and/ or 4'). In addition, it delays the undesirable decarbonylation of formic acid, which remains a challenge for using highconcentration or neat formic acid.³⁸ As formic acid is being consumed, PMe3 can be freed and recoordinate to cobalt to first form [(^{iPr}PP^{Me}P)Co(CO)(PMe₃)][(HCO₂)(HCO₂H)_x] (5) and then (iPrPPMeP)Co(CO)H (6) as the less active forms of the catalyst. Further degradation to $[(^{iPr}PP^{Me}P)Co(CO)_2]$ - $[(HCO_2)(HCO_2H)_x]$ (8), protonated phosphine ligands, and the insoluble cobalt formate leads to the death of the catalyst. Looking forward, there is great room for improvement in developing more efficient, robust, and selective catalysts for additive-free dehydrogenation of neat formic acid. This study shows that, to take advantage of the relatively high acidity of neat formic acid, it can be beneficial to incorporate a basic ancillary ligand in the catalyst design.

MATERIALS AND METHODS

All information pertaining to the materials and methods used in this study is provided in the Supporting Information.

ASSOCIATED CONTENT

5 Supporting Information

The Supporting Information is available free of charge at https://pubs.acs.org/doi/10.1021/acscatal.4c04109.

Experimental details, NMR and IR spectra of the cobalt complexes (PDF)

X-ray crystallographic information of 1 (CIF)

X-ray crystallographic information of 2 (CIF)

X-ray crystallographic information of 5 (CIF)

X-ray crystallographic information of 6 (CIF)

Accession Codes

CCDC 2366743–2366746 contain the supplementary crystallographic data for this paper. These data can be obtained free of charge via www.ccdc.cam.ac.uk/data_request/cif, or by emailing data_request/cif, or by contacting The Cambridge Crystallographic Data Centre, 12 Union Road, Cambridge CB2 1EZ, UK; fax: + 44 1223 336033

AUTHOR INFORMATION

Corresponding Author

Hairong Guan — Department of Chemistry, University of Cincinnati, Cincinnati, Ohio 45221-0172, United States; orcid.org/0000-0002-4858-3159; Email: hairong.guan@uc.edu

Authors

Bedraj Pandey – Department of Chemistry, University of Cincinnati, Cincinnati, Ohio 45221-0172, United States Jeanette A. Krause – Department of Chemistry, University of Cincinnati, Cincinnati, Ohio 45221-0172, United States

Complete contact information is available at: https://pubs.acs.org/10.1021/acscatal.4c04109

Author Contributions

The manuscript was written through contributions of all authors. All authors have given approval to the final version of the manuscript.

Notes

The authors declare no competing financial interest.

ACKNOWLEDGMENTS

We thank the National Science Foundation (NSF) Chemical Catalysis Program for support of this research project (CHE-2102192 and CHE-2349483) and the NSF MRI Program for support of the instrumentation used in this study, which includes a Bruker D8 Venture diffractometer (CHE-1625737) and a Bruker NEO400 MHz NMR spectrometer (CHE-1726092). We are also grateful to Professor Jianbing "Jimmy" Jiang (U of Cincinnati) and Mr. Pramod Tiwari (U of Cincinnati) for their assistance with GC analysis. B.P. thanks the University of Cincinnati for a Doctoral Enhancement Research Fellowship.

■ REFERENCES

(1) (a) Mellmann, D.; Sponholz, P.; Junge, H.; Beller, M. Formic Acid as a Hydrogen Storage Material — Development of Homogeneous Catalysts for Selective Hydrogen Release. *Chem. Soc. Rev.* **2016**, *45*, 3954—3988. (b) Eppinger, J.; Huang, K.-W. Formic Acid as a Hydrogen Energy Carrier. *ACS Energy Lett.* **2017**, *2*, 188—195. (c) Sordakis, K.; Tang, C.; Vogt, L. K.; Junge, H.; Dyson, P. J.; Beller, M.; Laurenczy, G. Homogeneous Catalysis for Sustainable Hydrogen Storage in Formic Acid and Alcohols. *Chem. Rev.* **2018**,

- 118, 372-433. (d) Onishi, N.; Laurenczy, G.; Beller, M.; Himeda, Y. Recent Progress for Reversible Homogeneous Catalytic Hydrogen Storage in Formic Acid and in Methanol. Coord. Chem. Rev. 2018, 373, 317-332. (e) Guo, J.; Yin, C. K.; Zhong, D. L.; Wang, Y. L.; Qi, T.; Liu, G. H.; Shen, L. T.; Zhou, Q. S.; Peng, Z. H.; Yao, H.; Li, X. B. Formic Acid as a Potential On-Board Hydrogen Storage Method: Development of Homogeneous Noble Metal Catalysts for Dehydrogenation Reactions. ChemSusChem 2021, 14, 2655-2681. (f) Dutta, I.; Chatterjee, S.; Cheng, H.; Parsapur, R. K.; Liu, Z.; Li, Z.; Ye, E.; Kawanami, H.; Low, J. S. C.; Lai, Z.; Loh, X. J.; Huang, K.-W. Formic Acid to Power towards Low-Carbon Economy. Adv. Energy Mater. 2022, 12, 2103799. (g) Kumar, A.; Daw, P.; Milstein, D. Homogeneous Catalysis for Sustainable Energy: Hydrogen and Methanol Economies, Fuels from Biomass, and Related Topics. Chem. Rev. 2022, 122, 385-441. (h) Solakidou, M.; Gemenetzi, A.; Koutsikou, G.; Theodorakopoulos, M.; Deligiannakis, Y.; Louloudi, M. Cost Efficiency Analysis of H2 Production from Formic Acid by Molecular Catalysts. Energies 2023, 16, 1723.
- (2) (a) Bernskoetter, W. H.; Hazari, N. Reversible Hydrogenation of Carbon Dioxide to Formic Acid and Methanol: Lewis Acid Enhancement of Base Metal Catalysts. *Acc. Chem. Res.* **2017**, *50*, 1049–1058. (b) Guan, C.; Pan, Y.; Zhang, T.; Ajitha, M. J.; Huang, K.-W. An Update on Formic Acid Dehydrogenation by Homogeneous Catalysis. *Chem. Asian J.* **2020**, *15*, 937–946. (c) Iglesias, M.; Fernández-Alvarez, F. J. Advances in Nonprecious Metal Homogeneously Catalyzed Formic Acid Dehydrogenation. *Catalysts* **2021**, *11*, 1288. (d) Onishi, N.; Kanega, R.; Kawanami, H.; Himeda, Y. Recent Progress in Homogeneous Catalytic Dehydrogenation of Formic Acid. *Molecules* **2022**, *27*, 455.
- (3) Demirci, U. B.; Miele, P. Chemical Hydrogen Storage: 'Material' Gravimetric Capacity *versus* 'System' Gravimetric Capacity. *Energy Environ. Sci.* **2011**, *4*, 3334–3341.
- (4) Kar, S.; Rauch, M.; Leitus, G.; Ben-David, Y.; Milstein, D. Highly Efficient Additive-Free Dehydrogenation of Neat Formic Acid. *Nat. Catal.* **2021**, *4*, 193–201.
- (5) (a) Holtzberg, F.; Post, B.; Fankuchen, I. The Crystal Structure of Formic Acid. *Acta Crystallogr.* **1953**, *6*, 127–130. (b) Chocholoušová, J.; Vacek, J.; Hobza, P. Potential Energy and Free Energy Surfaces of the Formic Acid Dimer: Correlated *ab initio* Calculations and Molecular Dynamics Simulations. *Phys. Chem. Chem. Phys.* **2002**, *4*, 2119–2122.
- (6) Celaje, J. J. A.; Lu, Z.; Kedzie, E. A.; Terrile, N. J.; Lo, J. N.; Williams, T. J. A Prolific Catalyst for Dehydrogenation of Neat Formic Acid. *Nat. Commun.* **2016**, *7*, 11308.
- (7) Cohen, S.; Borin, V.; Schapiro, I.; Musa, S.; De-Botton, S.; Belkova, N. V.; Gelman, D. Ir(III)-PC(sp³)P Bifunctional Catalysts for Production of H₂ by Dehydrogenation of Formic Acid: Experimental and Theoretical Study. *ACS Catal.* **2017**, *7*, 8139–8146.
- (8) Iturmendi, A.; Iglesias, M.; Munarriz, J.; Polo, V.; Passarelli, V.; Pérez-Torrente, J.; Oro, L. A. A Highly Efficient Ir-Catalyst for the Solventless Dehydrogenation of Formic Acid: the Key Role of an N-Heterocyclic Olefin. *Green Chem.* **2018**, *20*, 4875–4879.
- (9) (a) Wang, S.; Huang, H.; Roisnel, T.; Bruneau, C.; Fischmeister, C. Base-Free Dehydrogenation of Aqueous and Neat Formic Acid with Iridium(III) Cp*(dipyridylamine) Catalysts. *ChemSusChem* **2019**, *12*, 179–184. (b) Guo, L.; Li, Z.; Cordier, M.; Marchal, R.; Le Guennic, B.; Fischmeister, C. Noninnocent Ligands for Efficient Dehydrogenation of Aqueous and Neat Formic Acid under Base-Free Conditions. *ACS Catal.* **2023**, *13*, 13626–13637.
- (10) Related Cp*Ir complexes have been studied as catalysts for dehydrogenation of formic acid in aqueous solutions. For details, see: (a) Siek, S.; Burks, D. B.; Gerlach, D. L.; Liang, G.; Tesh, J. M.; Thompson, C. R.; Qu, F.; Shankwitz, J. E.; Vasquez, R. M.; Chambers, N.; Szulczewski, G. J.; Grotjahn, D. B.; Webster, C. E.; Papish, E. T. Iridium and Ruthenium Complexes of N-Heterocyclic Carbene- and Pyridinol-Derived Chelates as Catalysts for Aqueous Carbon Dioxide Hydrogenation and Formic Acid Dehydrogenation: The Role of the Alkali Metal. *Organometallics* 2017, 36, 1091–1106. (b) Kanega, R.; Ertem, M. Z.; Onishi, N.; Szalda, D. J.; Fujita, E.; Himeda, Y. CO₂

- Hydrogenation and Formic Acid Dehydrogenation Using Ir Catalysts with Amide-Based Ligands. *Organometallics* **2020**, *39*, 1519–1531.
- (11) Alrais, L.; Gholap, S. S.; Dutta, I.; Abou-Hamad, E.; Chen, B. W. J.; Zhang, J.; Hedhili, M. N.; Basset, J.-M.; Huang, K.-W. Highly Efficient Immobilized PN³P-Pincer Iridium Catalyst for Dehydrogenation of Neat Formic Acid. *Appl. Catal. B: Environ.* **2024**, *342*, 123439.
- (12) Hermosilla, P.; Urriolabeitia, A.; Iglesias, M.; Polo, V.; Casado, M. A. Efficient Solventless Dehydrogenation of Formic Acid by a CNC-Based Rhodium Catalyst. *Inorg. Chem. Front.* **2022**, *9*, 4538–4547
- (13) Bullock, R. M.; Chen, J. G.; Gagliardi, L.; Chirik, P. J.; Farha, O. K.; Hendon, C. H.; Jones, C. W.; Keith, J. A.; Klosin, J.; Minteer, S. D.; Morris, R. H.; Radosevich, A. T.; Rauchfuss, T. B.; Strotman, N. A.; Vojvodic, A.; Ward, T. R.; Yang, J. Y.; Surendranath, Y. Using Nature's Blueprint to Expand Catalysis with Earth-Abundant Metals. *Science* 2020, 369, No. eabc3183.
- (14) Scotti, N.; Psaro, R.; Ravasio, N.; Zaccheria, F. A New Cu-Based System for Formic Acid Dehydrogenation. *RSC Adv.* **2014**, *4*, 61514–61517.
- (15) Enthaler, S.; Brück, A.; Kammer, A.; Junge, H.; Irran, E.; Gülak, S. Exploring the Reactivity of Nickel Pincer Complexes in the Decomposition of Formic Acid to CO₂/H₂ and the Dehydrogenation of NaHCO₃ to HCOONa. *ChemCatChem.* **2015**, *7*, 65–69.
- (16) Pandey, B.; Krause, J. A.; Guan, H. Iron Dihydride Complex Stabilized by an All-Phosphorus-Based Pincer Ligand and Carbon Monoxide. *Inorg. Chem.* **2022**, *61*, 11143–11155.
- (17) (a) Xu, G.; Sun, H.; Li, X. Activation of sp³ Carbon—Hydrogen Bonds by Cobalt and Iron Complexes and Subsequent C–C Bond Formation. *Organometallics* **2009**, *28*, 6090–6095. (b) Federsel, C.; Ziebart, C.; Jackstell, R.; Baumann, W.; Beller, M. Catalytic Hydrogenation of Carbon Dioxide and Bicarbonates with a Well-Defined Cobalt Dihydrogen Complex. *Chem. Eur. J.* **2012**, *18*, 72–75. (c) Li, Y.; Krause, J. A.; Guan, H. Silane Activation with Cobalt on the POCOP Pincer Ligand Platform. *Organometallics* **2020**, *39*, 3721–3730. (d) Kuehn, M. A.; Fernandez, W.; Zall, C. M. Structure and Thermodynamic Hydricity in Cobalt(triphosphine)(monophosphine) Hydrides. *Inorg. Chem.* **2023**, *62*, 8505–8518. (e) Saha, S.; Krause, J. A.; Guan, H. C(sp)—H, S—H, and Sn—H Bond Activation with a Cobalt(I) Pincer Complex. *Inorg. Chem.* **2024**, *63*, 13689–13699.
- (18) Pandey, B.; Krause, J. A.; Guan, H. Methyl Effects on the Stereochemistry and Reactivity of PPP-Ligated Iron Hydride Complexes. *Inorg. Chem.* **2023**, *62*, 967–978.
- (19) Addison, A. W.; Rao, T. N.; Reedijk, J.; van Rijn, J.; Verschoor, G. C. Synthesis, Structure, and Spectroscopic Properties of Copper(II) Compounds Containing Nitrogen—Sulphur Donor Ligands; the Crystal and Molecular Structure of Aqua[1,7-bis(N-methylbenzimidazol-2'-yl)-2,6-dithiaheptane]copper(II) Perchlorate. *J. Chem. Soc., Dalton Trans.* 1984, 1349—1356.
- (20) Onishi, M. Decomposition of Formic Acid Catalyzed by Hydrido(phosphonite)cobalt(I) Under Photoirradiation. *J. Mol. Catal.* **1993**, 80, 145–149.
- (21) (a) Zhou, W.; Wei, Z.; Spannenberg, A.; Jiao, H.; Junge, K.; Junge, H.; Beller, M. Cobalt-Catalyzed Aqueous Dehydrogenation of Formic Acid. *Chem. Eur. J.* **2019**, 25, 8459–8464. (b) Tsai, C.-P.; Chen, C.-Y.; Lin, Y.-L.; Lan, J.-C.; Tsai, M.-L. Catalytic Dehydrogenation of Formic Acid Promoted by Triphos-Co Complexes: Two Competing Pathways for H₂ Production. *Inorg. Chem.* **2024**, 63, 1759–1773.
- (22) Lentz, N.; Aloisi, A.; Thuéry, P.; Nicolas, E.; Cantat, T. Additive-Free Formic Acid Dehydrogenation Catalyzed by a Cobalt Complex. *Organometallics* **2021**, *40*, 565–569.
- (23) Bielinski, E. A.; Lagaditis, P. O.; Zhang, Y.; Mercado, B. Q.; Würtele, C.; Bernskoetter, W. H.; Hazari, N.; Schneider, S. Lewis Acid-Assisted Formic Acid Dehydrogenation Using a Pincer-Supported Iron Catalyst. *J. Am. Chem. Soc.* **2014**, *136*, 10234–10237. (24) Ge, X.; Zhang, R.; Liu, P.; Liu, B.; Liu, B. Optimization and Control of Extractive Distillation for Formic Acid-Water Separation

- with Maximum-Boiling Azeotrope. Comput. Chem. Eng. 2023, 169, 108075.
- (25) (a) Fellay, C.; Dyson, P. J.; Laurenczy, G. A Viable Hydrogen-Storage System Based on Selective Formic Acid Decomposition with a Ruthenium Catalyst. *Angew. Chem., Int. Ed.* **2008**, *47*, 3966–3968. (b) Iguchi, M.; Guan, C.; Huang, K.-W.; Kawanami, H. Solvent Effects on High-Pressure Hydrogen Gas Generation by Dehydrogenation of Formic Acid Using Ruthenium Complexes. *Int. J. Hydrogen Energy* **2019**, *44*, 28507–28513. (c) Geri, J. B.; Ciatti, J. L.; Szymczak, N. K. Charge Effects Regulate Reversible CO₂ Reduction Catalysis. *Chem. Commun.* **2018**, *54*, 7790–7793.
- (26) Pandey, B.; Krause, J. A.; Guan, H. On the Demise of PPP-Ligated Iron Catalysts in the Formic Acid Dehydrogenation Reaction. *Inorg. Chem.* **2023**, *62*, 18714–18723.
- (27) (a) Jeletic, M. S.; Helm, M. L.; Hulley, E. B.; Mock, M. T.; Appel, A. M.; Linehan, J. C. A Cobalt Hydride Catalyst for the Hydrogenation of CO₂: Pathways for Catalysis and Deactivation. *ACS Catal.* **2014**, *4*, 3755–3762. (b) Burgess, S. A.; Grubel, K.; Appel, A. M.; Wiedner, E. S.; Linehan, J. C. Hydrogenation of CO₂ at Room Temperature and Low Pressure with a Cobalt Tetraphosphine Catalyst. *Inorg. Chem.* **2017**, *56*, 8580–8589.
- (28) Protonation of $({}^{Ph}PP^{Ph}P)CoH(PMe_3)$ $({}^{Ph}PP^{Ph}P) = PhP(CH_2CH_2PPh_2)_2)$ with $HBF_4\cdot OEt_2$ was shown to give the 4-coordinate complex $[({}^{Ph}PP^{Ph}P)Co(PMe_3)]BF_4$. For details, see ref 17d.
- (29) Basch, H.; Stevens, W. J. The Strong Hydrogen Bond in the Formic Acid Formate Anion System. *J. Am. Chem. Soc.* **1991**, *113*, 95–101.
- (30) Halpern, J.; Kemp, A. L. W. The Decarbonylation of Formic Acid by Ruthenium(II) Chloride. *J. Am. Chem. Soc.* **1966**, 88, 5147–5150.
- (31) Shin, J. H.; Churchill, D. G.; Parkin, G. Carbonyl Abstraction Reactions of Cp*Mo(PMe₃)₃H with CO₂, (CH₂O)_n, HCO₂H, and MeOH: the Synthesis of Cp*Mo(PMe₃)₂(CO)H and the Catalytic Decarboxylation of Formic Acid. *J. Organomet. Chem.* **2002**, 642, 9–15
- (32) Ito, K.; Bernstein, H. J. The Vibrational Spectra of the Formate, Acetate, and Oxalate Ions. *Can. J. Chem.* **1956**, *34*, 170–178.
- (33) (a) Kaufman, A.; Afshar, C.; Rossi, M.; Zacharias, D. E.; Glusker, J. P. Metal Ion Coordination in Cobalt Formate Dihydrate. *Struct. Chem.* 1993, 4, 191–198. (b) Thakur, N.; Pandey, M. D.; Pandey, R. Co(II)-Catalyzed Decarboxylation of Itaconic Acid Engendering Methacrylic Acid and Co(II)-MOFs for Structure Regulated Fluorescent Detection of Cations. *J. Solid State Chem.* 2019, 280, 120987.
- (34) (a) Li, K.; Olson, D. H.; Lee, J. Y.; Bi, W.; Wu, K.; Yuen, T.; Xu, Q.; Li, J. Multifunctional Microporous MOFs Exhibiting Gas/Hydrocarbon Adsorption Selectivity, Separation Capability and Three-Dimensional Magnetic Ordering. *Adv. Funct. Mater.* **2008**, *18*, 2205–2214. (b) Huh, H. S.; Lee, S. W. Unexpected Formation of the Cobalt-Formate Coordination Polymer [Co₃(HCO₂)₆]·dmf from Co(NO₃)₂ and 2,2'-Bipyridine-5,5'-dicarboxylic Acid in dmf-EtOH-H₂O. *Bull. Korean Chem. Soc.* **2008**, *29*, 2383–2389.
- (35) (a) Zou, X.; Zhang, F.; Thomas, S.; Zhu, G.; Valtchev, V.; Mintova, S. Co₃(HCOO)₆ Microporous Metal-Organic Framework Membrane for Separation of CO₂/CH₄ Mixtures. *Chem. Eur. J.* **2011**, 17, 12076–12083. (b) Wang, H.; Yao, K.; Zhang, Z.; Jagiello, J.; Gong, Q.; Han, Y.; Li, J. The First Example of Commensurate Adsorption of Atomic Gas in a MOF and Effective Separation of Xenon from Other Noble Gases. *Chem. Sci.* **2014**, *5*, 620–624.
- (36) Viertelhaus, M.; Adler, P.; Clérac, R.; Anson, C. E.; Powell, A. K. Iron(II) Formate [Fe(O₂CH)₂] •1/3HCO₂H: A Mesoporous Magnet Solvothermal Syntheses and Crystal Structures of the Isomorphous Framework Metal(II) Formates [M(O₂CH)₂]·n(Solvent) (M = Fe, Co, Ni, Zn, Mg). Eur. J. Inorg. Chem. 2005, 2005, 692–703.
- (37) Neary, M. C.; Parkin, G. Nickel-Catalyzed Release of H₂ from Formic Acid and a New Method for the Synthesis of Zerovalent Ni(PMe₃)₄. Dalton Trans. **2016**, 45, 14645–14650.

(38) Wakai, C.; Yoshida, K.; Tsujino, Y.; Matubayasi, N.; Nakahara, M. Effect of Concentration, Acid, Temperature, and Metal on Competitive Reaction Pathways for Decarbonylation and Decarboxylation of Formic Acid in Hot Water. *Chem. Lett.* **2004**, *33*, 572–573.